RAPID COMMUNICATIONS

PHYSICAL REVIEW B VOLUME 47, NUMBER 13 1 APRIL 1993-I

Investigation of giant magnetoresistance in concentrated and nanostructured alloys

Jian-Qing Wang, Peng Xiong, and Gang Xiao
Department of Physics, Brown University, Providence, Rhode Island 02912
(Received 10 November 1992; revised manuscript received 19 January 1993)

Magnetotransport and magnetic properties of Fe-Cu, Fe-Ag, Fe-Au, and Fe-Pt alloys were studied across a wide range of Fe volume fraction and at different annealing conditions. The giant magnetoresistance (GMR) effect was observed in Cu-, Ag-, and Au-based systems, peaking at an Fe volume fraction of about 15–20 %. The Hall effect was also measured, which yielded the electron mean free path. Thermal annealing increases the magnetic particle size and reduces resistivity due to magnetic scattering. The GMR and its dependence on magnetic field are well accounted for by an effective exchange interaction model.

Much attention has been paid to the giant magnetoresistance (GMR) effect observed in magnetic multilayers,[1–4] and recently, in granular alloys.[5,6] Besides its potential application in magnetic sensors, the primary interest in GMR has been focused on the mechanism of the anomalous magnetotransport property. It is generally agreed upon that GMR is a manifestation of the spin-dependent scattering. It is the extra resistance due to the scattering of electrons off nonaligned ferromagnetic components. In inhomogenous systems, like multilayered and granular systems, the spin-dependent scattering can take place at interfaces separating magnetic and nonmagnetic phases or inside the bulk. According to the quantum model of Levy, Zhang, and Fert,[4] in multilayered systems both interface and bulk scatterings are important. In granular systems, however, there is evidence[7] that the interface scattering plays a dominant role due to the enhanced surface-to-volume ratio of the magnetic ultrafine particles. Despite significant effort, the fundamental question as to the origin of the spin-dependent scattering remains uncertain. For the celebrated granular systems, in particular, both experimental and theoretical investigations are still in a primary stage where much effort is needed to characterize and understand the GMR effect.

In this paper, we report a systematic study of magnetotransport and magnetic properties of a series of Fe-based binary systems, i.e., Fe-Cu, Fe-Ag, Fe-Au, and Fe-Pt, with a wide range of Fe volume fraction ($0 \leq x \leq 100\%$). Our intention is to uncover common features with regard to GMR among these systems, and to search for uniqueness in each system. We have chosen the first three systems because the mutual solubility in each system is small or practically zero in equilibrium. Fe-Pt, on the other hand, does have many intermetallics, and serves as a good counterpart to the other systems. We found that, if it exists, the GMR effect is sensitive to the Fe content. Maximum GMR was found for the first three systems in the range $x \approx 15 - 20\,\%$. However, GMR was not observed in the Fe-Pt system. We also obtained the effective electron mean free path λ_{eff} for these systems. The value of λ_{eff} is rather small across each series. Annealing of Fe-Cu and Fe-Ag samples reduces the saturation field for GMR significantly and decreases the magnitude of magnetoresistance concurrently. We used an effective exchange interaction model to account for the magnetotransport properties, which explains well the observed features in MR.

The samples were fabricated by a magnetron cosputtering high vacuum system. Two of the three collimated cluster guns were loaded with a nonmagnetic metal and a Fe target, respectively. The background vacuum was lower than 1×10^{-7} Torr, and the Ar sputtering gas pressure was 4.0 mTorr. The volume fraction of each sample was set by the deposition rate of each component. Films of typical thickness 2000 Å were deposited on Si wafers at ambient temperature. The standard photolithography and wet-etching technique was used to pattern our samples for electrical measurement. Using a superconducting-quantum-interference-device magnetometer we characterized the magnetic properties of every system. The structure and phase information were derived from x-ray diffraction.

The measured resistivity ρ_{xx}, Hall resistivity ρ_{xy}, and magnetization at $T = 4.2$ K are presented in Fig. 1 for a representative sample from each series. These samples tend to have the largest magnetoresistance (MR) in each series. Relatively large MR values of $16 - 31\,\%$ are obtained in $Fe_{20}Cu_{80}$, $Fe_{13}Ag_{87}$, and $Fe_{15}Au_{85}$. The values of MR in Fig. 1 show a rather gradual decrease with magnetic field (H) up to the highest field ± 8 T in our measurement. It is noted that magnetic field is perpendicular to the sample plane. Comparing with the measured magnetization (lower panels) of each corresponding sample, we did not observe the simple M^2 law of MR as was uncovered in the Co-Cu granular system.[6] Furthermore, MR does not reach saturation even at the highest field. The Hall resistivity ρ_{xy} in Fig. 1 consists of an ordinary Hall component and an extraordinary Hall component, i.e., $\rho_{xy} = \rho_0 + \rho_s$, where $\rho_0 = R_0[H + 4\pi M(1 - D)]$ and

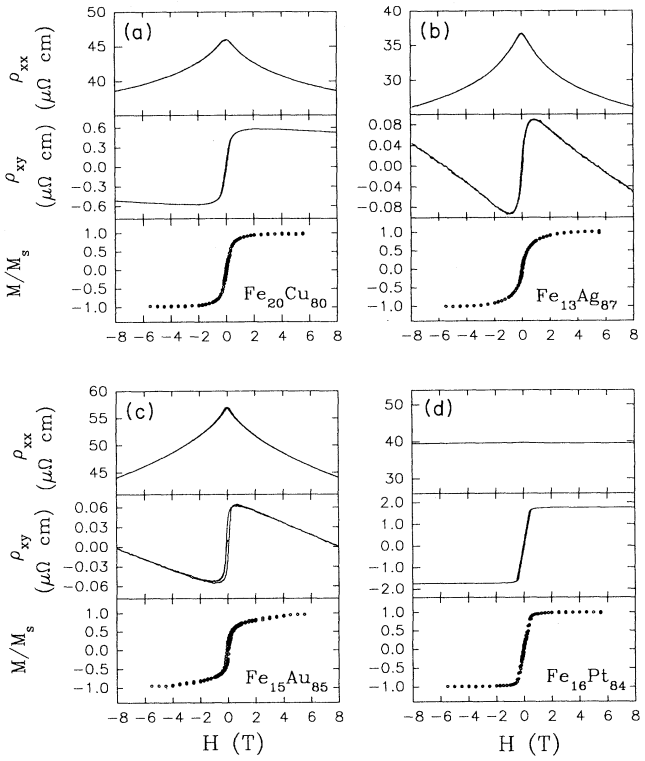

FIG. 1. Measured resistivity ρ_{xx} (upper panels), Hall resistivity ρ_{xy} (middle panels), and normalized magnetization M/M_s (lower panels) vs magnetic field at $T = 4.2$ K for $Fe_{10}Cu_{90}$ (a), $Fe_{13}Ag_{87}$ (b), Fe_{15} Au_{85} (c), and Fe_{16} Pt_{84} (d). (Subscripts are in units of vol %.). Note: The magnetic field is perpendicular to the sample plane.

$\rho_s = R_s 4\pi M$, D being the demagnetization factor. The cause of the ρ_s component is the left-right asymmetry in scattering. Since ρ_s is proportional to the magnetization, it directly reflects the state of magnetization at any given field.[7]

In sharp contrast to other series, the Fe_xPt_{100-x} series does not exhibit large MR. For comparison, we show the results of the $Fe_{16}Pt_{84}$ sample in Fig. 1(d). The sample is characterized by a small MR (< 1%), a large extraordinary Hall effect, and a well-defined saturation field. In fact, our sample with the lowest Fe volume fraction of 8% remains ferromagnetic in nature with a clear-cut saturation of magnetization above a critical field. In all other series, near the Fe-poor region, saturation of magnetization is gradual rather than abrupt, which is typical of dilute random magnetic systems lacking long-range order. It should also be pointed out that Fe induces a giant magnetic moment in the Pt matrix. This may be related to the destruction of GMR in the Fe-Pt series.

To find out the optimized GMR, we have studied the volume-fraction dependence of the magnetotransport properties. The results are shown in Fig. 2(a) for the Fe-Cu, Fe-Ag, and Fe-Au systems. The Fe volume fraction was determined from the composition and the bulk density of each component. This is to be consistent with the granular nature of our samples. There is evidence of magnetic cluster formation in as-sputtered samples as revealed from the transmission-electron-microscopy (TEM) and magnetic susceptibility measurement. In Fig. 2(a) GMR is defined as $[\rho_{xx}(0) - \rho_{xx}(8T)]/\rho_{xx}(0)$. Relatively large GMR values are present in the range $x < 40\%$, with GMR peaking at $x \approx 15 - 20\,\%$. Starting from the dilute limit, GMR rises as x increases, until a broad maximum is reached around $x \approx 15 - 20\,\%$. This behavior is attributed to the increasing concentration of magnetic scattering centers. After reaching the peak, GMR starts to decrease beyond $x \sim 20\%$. We believe that this is due to the increasing probability of coalescence of the Fe particles. Most of the Fe atoms or particles start to connect and form a cluster network. Long-range magnetic order is expected within the network, with the complication of magnetic domain formation. When the average domain size exceeds the coherent spin scattering length, the electrons may no longer experience the overall magnetic disorder. Therefore the field-induced magnetic disorder-order transformation, essential to GMR, becomes inactive on the electron transport. Consequently, GMR decreases in the Fe-rich region. We feel that the small MR in the Fe-Pt series is also caused by the existing long-range ferromagnetic order.

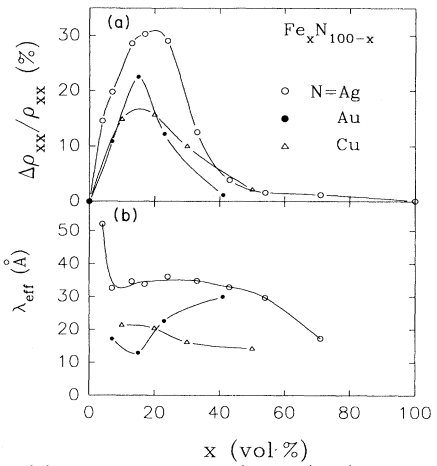

FIG. 2. (a) Values of GMR ($\Delta\rho_{xx}/\rho_{xx}$) vs the Fe volume fraction x for as-sputtered samples of Fe-Ag (open circles), Fe-Au (closed circles), and Fe-Cu (triangles). The lines are guide to the eyes. (b) The effective mean free paths of the corresponding samples derived from ρ_{xx} and ρ_{xy}. ($T = 4.2$ K.)

To set the scattering length scale, it is useful to examine the effective electron mean free path λ_{eff}. In fact, any theoretical model of GMR would depend on this length scale. By using the Drude formula $\rho_{xx} = m^* v_F / ne^2 \lambda_{\text{eff}}$, $R_0 = 1/nec$, and $v_F = \hbar\sqrt[3]{3\pi^2 n}/m^*$, one can derive λ_{eff}. We present in Fig. 2(b) the values of λ_{eff} for all three systems. One observes that λ_{eff} is short (20 $\sim$ 35 Å). This implies that the cluster size should be around 20 $\sim$ 35 Å, because the dominant scattering mechanism is due to grain boundary disorder. We have characterized the structure of these systems by x-ray diffraction. Under equilibrium, Fe is partially soluble in Au ($x < 5\%$) with no intermetallics. However, practically no mutual solubilities are allowed between Fe and Ag (or Cu). In as-sputtered samples, x-ray analysis of the Fe-Au series

TABLE I. The values of GMR ($\Delta\rho_{xx}/\rho_{xx}$), $\Delta\rho_{xx}$ (change in ρ_{xx} up to $H = 8$ T), and $\rho_{xx}(0)$ (zero field resistivity) for $Fe_{13}Ag_{87}$ and $Fe_{10}Cu_{90}$ (annealed at various temperature T_A; RT represents as-sputtered samples).

	T_A	RT	250 °C	325 °C	400 °C	475 °C
$Fe_{13}Ag_{87}$	GMR (%)	28.7	36.5	15.4	6.4	0.1
	$\Delta\rho_{xx}$ ($\mu\Omega$ cm)	10.51	5.89	1.363	0.328	0.005
	ρ_{xx} ($\mu\Omega$ cm)	36.68	16.12	8.83	5.13	4.03
$Fe_{10}Cu_{90}$	GMR (%)	14.9	13.9	11.9	3.4	
	$\Delta\rho_{xx}$ ($\mu\Omega$ cm)	4.440	1.765	1.304	0.248	
	ρ_{xx} ($\mu\Omega$ cm)	29.77	12.73	10.94	7.31	

indicated that metastable fcc alloys form up to $x = 60\%$. Similarly, Fe-Cu samples have metastable fcc structure up to $x = 50\%$. Thermal annealing of $Fe_{50}Cu_{50}$ showed that distinctive phase separation appeared above 325 °C. Our results are consistent with literature on sputtered Fe-Cu and Fe-Au.[8] For the Fe-Ag system, the structural assessment was less conclusive due to overlapping spectral lines of Fe and Ag, and the much smaller atomic number Z of Fe than that of Ag, causing the signal from the Fe phase, if any, to be harder to detect. In general, it is difficult to detect small clusters of Fe ($\sim$ 10 Å) in the Cu, Ag, or Au matrix, particularly in the Fe-poor region. TEM results on some as-sputtered Fe-Ag samples indicated the existence of very fine grains ($\sim$ 20 Å). The estimated grain size is about 30 – 60 Å from the width of the x-ray diffraction lines. We note that except for Fe-Pt where concentrated alloys are formed, the phase-separated Fe-Ag, Cu, Au series may consist of three phases, i.e., pure host, spin glass with Fe impurity, and phase-separated Fe. In Fe-Ag, Cu series, the spin glass phase contains a very minute amount of Fe particularly in annealed samples, because solubilities of Fe in both Ag and Cu are extremely low. However, the spin glass phase in Fe-Au may contain a few percent of Fe. But these differences have little effect qualitatively on the universal behavior of GMR shown in Fig. 2(a).

To assess the effect of cluster size on GMR, thermal annealing on some Fe-Ag and Fe-Cu samples was carried out under a high vacuum of 1×10^{-7} Torr and at various temperatures T_A for 15 min. In Fig. 3(a), we show the MR of $Fe_{13}Ag_{87}$ treated at different T_A. The GMR values and the absolute changes in resistivity $\Delta\rho_{xx} = \rho(0T) - \rho(8T)$ are listed in Table I for $Fe_{13}Ag_{87}$ and $Fe_{10}Cu_{90}$. For $Fe_{13}Ag_{87}$, we notice that GMR initially increases at low T_A and then decreases at subsequent higher T_A's, but $\Delta\rho_{xx}$ decreases monotonically with increasing T_A. The initial increase in GMR is due to the reduction of $\rho(0\ \mathrm{T})$ upon annealing, while the monotonic decrease of $\Delta\rho_{xx}$ is caused by the enlarged particle due to annealing. Larger particles have reduced surface-to-volume ratio, hence, a diminished contribution of interface magnetic scattering. This effect has been carefully examined and discussed in our earlier work for Co-Ag system.[7] TEM imaging of the annealed samples of $Fe_{20}Ag_{80}$ showed that phase separation occurred and grain size increased monotonically with T_A. At subsequent T_A of 250, 325, 400, and 475 °C, we observed the average grain size of 85, 140, 220, and 310 Å, respectively.

Another salient feature in Fig. 3(a) is the evolution of the MR saturation field with T_A. The MR of the as-sputtered sample is similar to the MR of some dilute

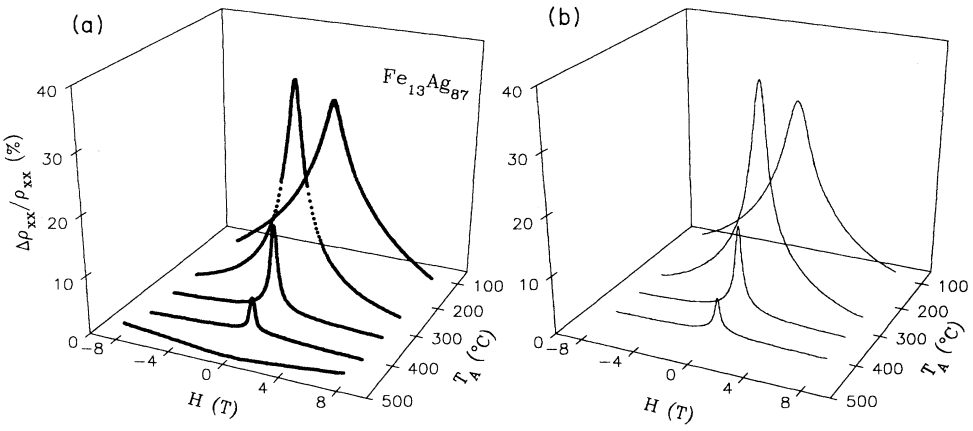

FIG. 3. (a) Measured MR vs H at $T = 4.2$ K of $Fe_{13}Ag_{87}$ annealed at various temperatures T_A. (b) Theoretical fitted results of MR vs H using the EEI model.

magnetic alloys, e.g., FeAu.[9] The saturation of MR is difficult to achieve even at a high H. However, the MR saturation becomes easier for samples annealed at higher T_A. As shown in Fig. 3(a), the saturation field H_s decreases dramatically with increasing T_A, which has the effect of enlarging the particle. This interesting correlation between H_s and the particle size is one of the most important characteristics of GMR in granular systems.

We have attempted to understand this correlation by using an effective exchange interaction (EEI) model, which has successfully explained the MR in dilute magnetic systems.[10] We will only discuss briefly the results of this model and leave the detailed analysis to a future paper. In this model, the scattering potential is assumed to be

$$H_1 = V - 2J\mathbf{s}\cdot\mathbf{S} \tag{1}$$

where V is the spin-independent scattering potential, and J the effective exchange interaction between the spin $\mathbf{s}$ of a conduction electron and the spin $\mathbf{S}$ of a magnetic scatterer. Under (1), the spin-dependent ($\pm$) electron scattering rate is found to be dependent on the global magnetization $M(H)$ of a sample in an applied field H

$$\frac{1}{\tau_\pm} = A[1 + BM \mp CM], \tag{2}$$

$$M = -\frac{(2S+1)}{2}\coth\{\tfrac{2S+1}{2}\alpha\} + \tfrac{1}{2}\coth\{\alpha/2\}, \tag{3}$$

where

$$\alpha = g\mu_B H/k_B T, \tag{4}$$

$$A = \frac{mk_F N_i}{\pi\hbar^3}[V^2 + J^2 S(S+1)], \tag{5}$$

$$B = (J/V)^2 \tanh(\alpha/2)/[1 + (J/V)^2 S(S+1)], \tag{6}$$

$$C = 2(J/V)/[1 + (J/V)^2 S(S+1)]. \tag{7}$$

N_i in relation (5) is the number of scatterers in the sample. In deriving the above expressions, both elastic and inelastic (spin-flipping) scattering processes are considered.[10] g is the spectroscopic splitting factor. If conduction electrons of both spins are equally populated, we obtain resistivity as

$$\rho_{xx} = \rho_0\left[(1 + BM) - \frac{C^2M^2}{1 + BM}\right], \tag{8}$$

$$\rho_0 = m^* A/ne^2. \tag{9}$$

As can be seen from relation (3) and (8), the field dependence of M and ρ_{xx} is controlled by $\alpha = g\mu_B H/k_B T$ and S, i.e., the ratio of the magnetic energy of a particle to the thermal energy. A larger magnetic moment (or particle size) results in easier saturation of both M and ρ_{xx}. This provides a qualitative explanation for the correlation between H_s and T_A obtained in Fig. 3(a). With relations (3) and (8), we have fitted the data in Fig. 3(a) with only a few adjustable parameters, S and J/V. The fitted results are shown in Fig. 3(b). Indeed, the theoretical curves reproduce the experimental data rather well. The fitted values of S and J/V range from 6.6 and 0.63 for the as-sputtered sample to 36.9 and 0.05 for the annealed sample at 400 °C, respectively. The main effect of annealing is to increase the effective spin S which causes the reduction in H_s. Since we limit our model analysis to samples with identical volume fraction but annealed at different temperatures, the main effect on the scattering is due to changes in particle size, not due to coalescence of particles.

In conclusion, we have carried out a systematic study on the GMR effect in Fe-Cu, Fe-Ag, Fe-Au, and Fe-Pt systems. Large MR values were observed in the first three systems with an optimal range of $x \approx 15 - 20\,\%$. The measurement of both ρ_{xx} and ρ_{xy} has provided the effective electron mean free path, which is relatively short ($20 \sim 35$ Å). The EEI model explains the saturation process of MR for samples annealed at different T_A.

This work was supported by National Science Foundation Grant Nos. DMR-9024402 and DMR-9022033. G.X. wishes to thank the A.P. Sloan Foundation for partial financial support.

[1] M. N. Baibich, J. M. Broto, A. Fert, F. Nguyen Van Dau, F. Petroff, P. Eitenne, G. Creuzet, A. Friederich, and J. Chazelas, Phys. Rev. Lett. **61**, 2472 (1988).

[2] S. S. P. Parkin, N. More, and K. P. Roche, Phys. Rev. Lett. **64**, 2304 (1990).

[3] R. E. Camley and J. Barnaś, Phys. Rev. Lett. **63**, 664 (1989); A. Barthélémy and A. Fert, Phys. Rev. B **43**, 13124 (1991).

[4] P. M. Levy, S. Zhang, and A. Fert, Phys. Rev. Lett. **65**, 1643 (1990).

[5] A. E. Berkowitz, J. R. Mitchell, M. J. Carey, A. P. Young, S. Zhang, F. E. Spada, F. T. Parker, A. Hutten, and G. Thomas, Phys. Rev. Lett. **68**, 3745 (1992).

[6] J. Q. Xiao, J. S. Jiang, and C. L. Chien, Phys. Rev. Lett. **68**, 3749 (1992).

[7] P. Xiong, Gang Xiao, J. Q. Wang, J. Q. Xiao, J. S. Jiang, and C. L. Chien, Phys. Rev. Lett. **69**, 3220 (1992).

[8] J. R. Childress, C. L. Chien, and M. Nathan, Appl. Phys. Lett. **56**, 95 (1990); W. Felsch, Z. Angew. Phys. **29**, 217 (1970).

[9] H. Rohrer, Phys. Rev. **174**, 583 (1968).

[10] T. Van Peski-Tinbergen and A. J. Dekker, Physica **29**, 917 (1963).